An improved surface passivation method for single-molecule studies

Boyang Hua[1], Kyu Young Han[2–4], Ruobo Zhou[2,3,10], Hajin Kim[5,6], Xinghua Shi[4,7], Sanjaya C Abeysirigunawardena[8], Ankur Jain[1], Digvijay Singh[1], Vasudha Aggarwal[1], Sarah A Woodson[8,9] & Taekjip Ha[1–4,7]

We report a surface passivation method based on dichlorodimethylsilane (DDS)–Tween-20 for *in vitro* single-molecule studies, which, under the conditions tested here, more efficiently prevented nonspecific binding of biomolecules than the standard poly(ethylene glycol) surface. The DDS–Tween-20 surface was simple and inexpensive to prepare and did not perturb the behavior and activities of tethered biomolecules. It can also be used for single-molecule imaging in the presence of high concentrations of labeled species in solution.

During the past two decades, single-molecule techniques have been greatly advanced and widely applied to biological sciences[1–3]. Nowadays, using wide-field fluorescence microscopy[4], one can routinely record signals in parallel from hundreds of single biomolecules tethered to a surface. One of the many merits of single-molecule techniques is that it reveals intermediate states as well as heterogeneity in biomolecules that are otherwise hidden in conventional ensemble-averaging measurements. However, a continuing methodological challenge is that nonspecifically bound biomolecules on the imaging surface are difficult to filter out during analysis of the target molecules and sometimes alter results by their contribution to the overall statistical analysis.

Poly(ethylene glycol) (PEG) passivation[5,6] and protein blocking[7] are two widely used surface passivation methods in single-molecule studies. However, the PEG surface typically is able to reject nonspecific adhesion of biomolecules only at low nanomolar concentrations, and the protein-blocking method is even less effective[8]. This concentration range is too low for many physiologically relevant biomolecular interactions to take place because weak and transient interactions often exhibit dissociation constants (K_D) in the micromolar range[9]. Several optical measurement techniques have been developed to detect single fluorophores at higher concentrations[10,11], but these methods cannot achieve their maximum utility without better passivated surfaces.

Here we report an improved surface passivation method for single-molecule studies that can reduce nonspecific adsorption of biomolecules by typically tenfold and up to 30-fold, depending on the system under study, as compared to the PEG surface, while keeping biomolecular activities intact. Our method is also much less expensive in terms of time and reagent cost.

Previous work suggested that additional passivation with polysiloxane and Tween-20 on a PEG surface improves surface passivation[12]. However, this approach extends the PEG surface preparation time by an additional 16 h and leads to strong green background fluorescence requiring overnight laser bleaching. We were inspired to explore another type of previously reported surface that was passivated with hydrophobic coating materials and the surfactant F-127 (ref. 13). We tested eight different combinations of hydrophobic coating silanes and surfactants using Cy5-labeled DNA polymerase DinB[14] (**Supplementary Fig. 1**). We found that DDS–Tween-20 (DT20) had better passivation capacity, shorter preparation time and lower cost than other combinations.

Tween-20 that self-assembled onto the DDS-coated surface served as the passivation layer, and biotinylated bovine serum albumin (BSA) adsorbed before Tween-20 treatment was used to present biotin for tethering target biomolecules through the biotin-NeutrAvidin interaction (**Fig. 1a**). The autofluorescence of Tween-20 was negligible compared to that of typical organic fluorophores used for single-molecule imaging. The DT20 and PEG surfaces had similar densities of fluorescence impurities, although we observed some diffusion of impurities on the DT20 surface (**Supplementary Fig. 2** and **Supplementary Video 1**). We performed tests with fluorophore-labeled proteins or nucleic acids and counted the number of fluorescent spots per imaging area (~2,500 μm^2) as the indicator of the level of nonspecific binding. As a standard protocol for comparison, we washed out free biomolecules after incubation for spot counting (Online Methods). Compared to the PEG surface, the DT20 surface consistently yielded much lower nonspecific-binding spot counts for Cy5-labeled DinB over a wide protein concentration range (from 5 nM to 200 nM) at pH 8.0 (**Fig. 1b**). The improvement factor was about 30-fold regardless of the presence of NeutrAvidin, so a potential effect of different NeutrAvidin surface densities on the

[1]Center for Biophysics and Computational Biology, University of Illinois at Urbana-Champaign, Urbana, Illinois, USA. [2]Department of Physics, University of Illinois at Urbana-Champaign, Urbana, Illinois, USA. [3]Center for the Physics of Living Cells, University of Illinois at Urbana-Champaign, Urbana, Illinois, USA. [4]Howard Hughes Medical Institute, Urbana, Illinois, USA. [5]School of Life Sciences, Ulsan National Institute of Science and Technology, Ulsan, Republic of Korea. [6]Center for Soft and Living Matter, Institute for Basic Science, Ulsan, Republic of Korea. [7]Institute for Genomic Biology, University of Illinois at Urbana-Champaign, Urbana, Illinois, USA. [8]T.C. Jenkins Department of Biophysics, Johns Hopkins University, Baltimore, Maryland, USA. [9]Program in Cell, Molecular, Developmental Biology, and Biophysics (CMDB), Johns Hopkins University, Baltimore, Maryland, USA. [10]Present address: Department of Chemistry and Chemical Biology, Harvard University, Cambridge, Massachusetts, USA. Correspondence should be addressed to T.H. (tjha@illinois.edu).

RECEIVED 24 DECEMBER 2013; ACCEPTED 24 AUGUST 2014; PUBLISHED ONLINE 12 OCTOBER 2014; DOI:10.1038/NMETH.3143

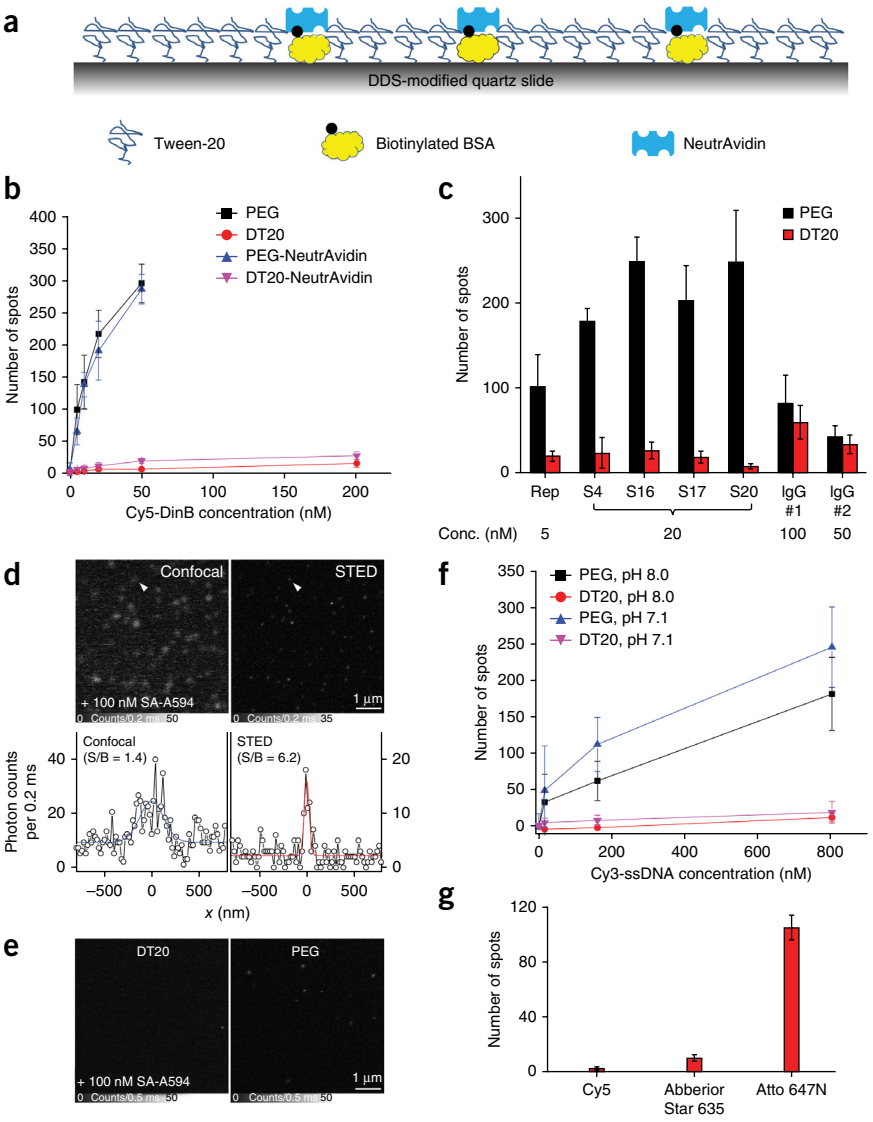

Figure 1 | Surface passivation with DT20. (**a**) Schematic of the DT20 surface. (**b**) Nonspecific binding of Cy5-labeled DinB on the DT20 and PEG surfaces, with and without NeutrAvidin, measured by the average surface spot counts of DinB over an imaging area of 2,500 µm^2 at different concentrations of DinB. (**c**) Surface spot counts over an imaging area of 2,500 µm^2 for nonspecific binding of seven different proteins to PEG and DT20 surfaces. Rep helicase was labeled with Cy5 and tested at pH 8.0; four ribosomal proteins (S4, S16, S17 and S20) were labeled with Cy3 and tested at pH 7.6; IgG #1 (611-701-127, Rockland) and IgG #2 (A-11004, Invitrogen) were labeled with Alexa 647 and Alexa 568, respectively, and tested at pH 8.0. (**d**) Top, fluorescence images of DT20 surface–immobilized streptavidin–Alexa 594 (SA-A594) imaged by confocal and STED microscopy in the presence of 100 nM diffusing SA-A594. Bottom, line profiles of single SA-A594 indicated by the white arrowheads in the top panels. S/B, signal-to-background ratio. The blue and red solid lines are Gaussian fits of profiles, and the maximum intensity is located at $x = 0$. (**e**) Nonspecific-binding tests of the DT20 and PEG surfaces incubated with 100 nM SA-A594, imaged by STED microscopy. (**f**) Nonspecific binding of Cy3-labeled ssDNA at different concentrations, measured at pH 8.0 and pH 7.1. (**g**) Surface spot counts over an imaging area of 2,500 µm^2 for nonspecific binding of 500 nM ssDNA (18 nt) labeled with three different fluorophores. Error bars, s.d. ($n = 5$–20).

PEG versus DT20 surfaces can be ruled out as the source of the large difference in surface passivation (**Supplementary Fig. 3**). The improvement in passivation capacity was due to the self-assembled Tween-20 layer rather than the biotinylated BSA; without additional Tween-20 treatment, the DDS-BSA surface had a much poorer passivation capacity (**Supplementary Fig. 4**). Successive binding tests on the same DT20 surface area indicated that nonspecific binding occurred at random positions, although we cannot rule out the possibility of surface defects that preferentially attract proteins (**Supplementary Fig. 5**).

In addition to using DinB, we also conducted nonspecific-binding tests for seven other proteins (Rep helicase; ribosomal proteins S4, S16, S17 and S20; and two antibodies) (**Fig. 1c** and **Supplementary Fig. 6**). With the exception of the antibodies, compared to the PEG surface, the DT20 surface exhibited at least fivefold reduction in nonspecific binding. We found that IgGs were not highly adhesive to the PEG surface, so the DT20 and PEG surfaces performed roughly the same in the IgG nonspecific-binding tests.

We next performed nonspecific-binding tests in the presence of high concentrations of fluorescent species in solution. A subdiffraction-limited focal spot generated by a stimulated emission depletion (STED) microscope enabled us to image surface-tethered single molecules with high signal-to-background ratio in the presence of 100 nM streptavidin labeled with Alexa 594 (ref. 15; **Fig. 1d**). In addition, the STED images obtained with labeled proteins in solution showed that the DT20 surface had reduced nonspecific binding of streptavidin and protein G B1 domain (**Fig. 1e** and **Supplementary Fig. 7**).

We also tested the nonspecific binding of a Cy3-labeled ssDNA (34 nt). The DT20 surface prevented nonspecific absorption of ssDNA tenfold more effectively than the PEG surface under the two pH conditions we tested (pH 7.1 and pH 8.0; **Fig. 1f** and **Supplementary Fig. 8**) and maintained its passivation capacity with $MgCl_2$ concentrations up to 80 mM (**Supplementary Fig. 9**). We tested additional fluorophores (Cy5, Abberior Star 635 and Atto 647N) linked to 18-nt ssDNA and found that each except Atto 647N displayed minimal nonspecific binding (**Fig. 1g**). Atto 647N–labeled ssDNA bound to the surface and diffused rapidly (**Supplementary Video 2**), likely because it was incorporated into the surfactant layer, consistent with severe nonspecific adsorption of Atto 647N to lipid bilayers reported previously[16]. This suggests that other fluorophores that are known to strongly interact with the lipid bilayers[16], such as nonsulfonated Cy3, would be unsuitable for use on the DT20 surface if the fluorophores were conjugated to short DNA.

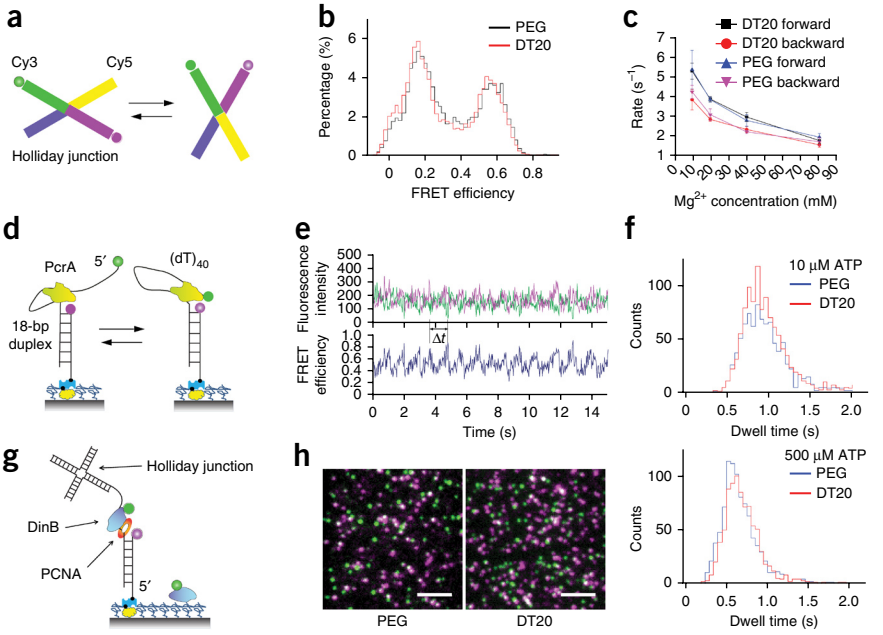

Figure 2 | Comparative analyses of biomolecular activities on the DT20 and PEG surfaces. (**a**) Holliday junction (HJ) dynamics monitored by FRET. (**b**) FRET histograms of single HJs obtained at 80 mM Mg^{2+}. (**c**) HJ transition rates as a function of Mg^{2+} concentration. Error bars, s.d. (n = 3). (**d**) PcrA reeling causes the looping of the 5′ ssDNA tail. (**e**) Representative intensity and FRET-time traces of 5′ ssDNA tail looping (green and magenta for Cy3 and Cy5 signals, respectively). (**f**) Δt histograms obtained for PcrA translocation at 10 μM ATP (top) and 500 μM ATP (bottom). (**g**) The FRET signal distinguishes PCNA-bound DinB from nonspecifically bound DinB. An HJ structure is used to prevent PCNA from sliding off the ssDNA region[14]. (**h**) Fluorescence images of DinB-PCNA interaction showing the overlay of the Cy3 (green) and Cy5 (magenta) channels for both surfaces. Scale bars, 4.5 μm.

To test the biocompatibility of the DT20 surface with proteins and nucleic acids, we systematically compared single-molecule data sets obtained on the DT20 and PEG surfaces. First, we measured the spontaneous transitions between the two stacked conformations of DNA Holliday junction (HJ) molecules[17] using single-molecule fluorescence resonance energy transfer (FRET)[18] (**Fig. 2a**). Single HJ FRET-time traces obtained from both surfaces showed clear two-state transitions (**Supplementary Fig. 10**). The histograms of FRET efficiencies were nearly identical between the two surfaces in terms of the peak positions of the high and low FRET conformations and their ratio (**Fig. 2b** and **Supplementary Fig. 11**). The transition rates between the high and low FRET conformations are known to increase with decreasing magnesium concentrations[17]; our analysis confirmed this and showed no substantial difference in the transition rates between the two surfaces (**Fig. 2c**).

We next measured the repetitive looping activity of PcrA helicase on a partial duplex DNA with a 5′ ssDNA overhang[19] (**Fig. 2d**). We observed the same sawtooth-shaped FRET-time traces, resulting from the repetitive PcrA translocation on the ssDNA overhang, as those previously obtained with the PEG surface under the same conditions[19] (**Fig. 2e**). To compare the translocation speed of PcrA on the two surfaces, we plotted the histograms of time intervals between two adjacent sudden drops (Δt) obtained from many single-molecule FRET-time traces at two ATP concentrations (**Fig. 2f**). Δt histograms obtained using the two surfaces gave almost identical distributions at each ATP concentration, indicating that the ssDNA translocation speed of PcrA was not much affected by the DT20 surface. Tests with the ribosomal protein S4-rRNA complex also confirmed the applicability to RNA-protein interactions[20] (**Supplementary Fig. 12**).

As a model system for protein-protein interactions, we examined the binding of DNA polymerase DinB to its processivity factor PCNA clamp at the concentration of 4 nM (ref. 14; **Fig. 2g**). It has been shown that PCNA can promote the DinB loading to DNA at the replication fork through PCNA-DinB interactions[14], so the formation of a ternary DinB-PCNA-DNA complex should result in a colocalized spot showing middle to high FRET value. In the Cy3 (green) and Cy5 (magenta) overlay images for both the PEG and DT20 surfaces, we observed white- to magenta-colored spots, indicating the PCNA-DinB interaction was preserved on the DT20 surface (**Fig. 2h**). A lower density of spots on the PEG surface was due to a lower DNA coverage. Green spots were due to DinB bound to DNA with inactive or missing Cy5 because at ~4 nM, nonspecifically adsorbed DinB exists at a much lower surface density (**Fig. 1b**).

In this work, we immobilized biomolecules through biotinylated BSA that is nonspecifically adsorbed to the DDS-coated surface before Tween-20 self-assembly. This method is compatible with long-term imaging because less than 20% of the biotinylated BSA detached from the DT20 surface over 2 h (**Supplementary Fig. 13**). To test how long the noncovalently self-assembled Tween-20 layer may last, we measured nonspecific binding of 500 nM Cy3-labeled ssDNA (34 nt) at pH 8.0 at different time points after the Tween-20 treatment. After 5 h, the DT20 surface did not lose much effectiveness in rejecting nonspecific binding (**Supplementary Fig. 14**).

In summary, we have devised and characterized a surface passivation method for single-molecule biological studies that substantially reduces nonspecific binding while maintaining native biomolecule activities. Because this method avoids the long PEGylation step[5] and uses inexpensive reagents, it is also time and cost effective. The DT20 surface provides a useful alternative to the PEG method and extends the reach of the powerful *in vitro* single-molecule experimental tools.

METHODS

Methods and any associated references are available in the online version of the paper.

Note: Any Supplementary Information and Source Data files are available in the online version of the paper.

ACKNOWLEDGMENTS

We thank B. Leslie, S. Syed, T. Ngo, F. Tritschler and Q. Xu for their helpful comments in data analyses and manuscript preparation; J. Guan, C. Yu and S. Granick for the helpful discussions and for generously letting us use the oxygen plasma cleaning machine and Piranha fume hood; T. Le of the H. Kim

laboratory at Georgia Institute of Technology and H.R. Koh of the S. Myong laboratory at the University of Illinois for performing independent tests of our protocols; and W. Cheng (University of Michigan) for providing the Alexa 594–labeled protein G B1 domain sample. This work was supported by a US National Science Foundation grant (PHY 1430124 to T.H.) and US National Institutes of Health grants (GM065367 and AG042332 to T.H. and GM60819 to S.A.W.). T.H. is also supported by the Howard Hughes Medical Institute.

AUTHOR CONTRIBUTIONS

B.H. and T.H. designed the project; B.H., K.Y.H., R.Z., H.K. and X.S. performed the experiments; S.C.A. and S.A.W. provided the S4-rRNA complex and three other ribosomal protein samples; B.H., K.Y.H., R.Z., H.K., X.S., A.J., D.S., V.A. and T.H. analyzed the data; and B.H., K.Y.H., R.Z., H.K., X.S. and T.H. wrote the manuscript.

COMPETING FINANCIAL INTERESTS

The authors declare no competing financial interests.

1. Kim, H. & Ha, T. *Rep. Prog. Phys.* **76**, 016601 (2013).
2. Patterson, G., Davidson, M., Manley, S. & Lippincott-Schwartz, J. *Annu. Rev. Phys. Chem.* **61**, 345–367 (2010).
3. Xie, X.S., Choi, P.J., Li, G.-W., Lee, N.K. & Lia, G. *Annu. Rev. Biophys.* **37**, 417–444 (2008).
4. Funatsu, T., Harada, Y., Tokunaga, M., Saito, K. & Yanagida, T. *Nature* **374**, 555–559 (1994).
5. Ha, T. *et al. Nature* **419**, 638–641 (2002).
6. Heyes, C.D., Groll, J., Möller, M. & Nienhaus, G.U. *Mol. Biosyst.* **3**, 419–430 (2007).
7. Jeyachandran, Y.L., Mielczarski, J.A., Mielczarski, E. & Rai, B. *J. Colloid Interface Sci.* **341**, 136–142 (2010).
8. Visnapuu, M.-L., Duzdevich, D. & Greene, E.C. *Mol. Biosyst.* **4**, 394–403 (2008).
9. van Oijen, A.M. *Curr. Opin. Biotechnol.* **22**, 75–80 (2011).
10. Loveland, A.B., Habuchi, S., Walter, J.C. & van Oijen, A.M. *Nat. Methods* **9**, 987–992 (2012).
11. Elting, M.W. *et al. Opt. Express* **21**, 1189–1202 (2013).
12. Revyakin, A. *et al. Genes Dev.* **26**, 1691–1702 (2012).
13. Helenius, J., Brouhard, G., Kalaidzidis, Y., Diez, S. & Howard, J. *Nature* **441**, 115–119 (2006).
14. Shi, X. *et al. Nat. Methods* **9**, 499–503 (2012).
15. Han, K.Y. *et al. Nano Lett.* **9**, 3323–3329 (2009).
16. Hughes, L.D., Rawle, R.J. & Boxer, S.G. *PLoS ONE* **9**, e87649 (2014).
17. McKinney, S.A., Déclais, A.-C., Lilley, D.M.J. & Ha, T. *Nat. Struct. Biol.* **10**, 93–97 (2002).
18. Ha, T. *et al. Proc. Natl. Acad. Sci. USA* **93**, 6264–6268 (1996).
19. Park, J. *et al. Cell* **142**, 544–555 (2010).
20. Kim, H. *et al. Nature* **506**, 334–338 (2014).

ONLINE METHODS

Preparation of the DDS-coated surface[13]. The slides and coverslips cleaning procedure was the same as that for the regular PEG slides[5]. No prolonged burning was used in order to prevent dehydration of the surface hydroxyl groups[21]. The clean slides and coverslips were dried thoroughly with N_2 and placed in a dry glass slide holder. The slide holder was rinsed twice with hexane (Fisher Chemical, Spectranalyzed) in a fume hood. 75 ml hexane were added to the holder followed by the injection of ~0.05% (v/v) dichlorodimethylsilane (DDS, Sigma-Aldrich, >99.5%) using a 1-ml syringe with needle. DDS was injected quickly with the needle tip under hexane to avoid air contact. Then the holder was covered with its cap and wrapped tightly with aluminum foil. The holder was kept shaking gently at room temperature for 1–1.5 h. After the hexane solution was dumped to a designated hexane-DDS mixture waste bottle, the slides and coverslips were rinsed and sonicated with hexane for 1 min. The rinse and sonication step was repeated two more times. The slides and coverslips were dried with N_2 and placed in 50-ml Falcon tubes (BD). The tube in a food-saver bag was vacuum sealed and stored at −20 °C. A detailed protocol is available (**Supplementary Protocol**).

Using the DT20 slides. The slides and coverslips were warmed up to room temperature before use. Then they were assembled into flow chambers in the same manner as for the regular PEG slides. 50 µl 0.2 mg/ml biotinylated BSA (A8549, Sigma) in T50 buffer (20 mM Tris and 50 mM NaCl at pH 8.0) were flowed in each channel and incubated for 5 min. 100 µl 0.2% Tween-20 (Fisher BioReagents) in T50 buffer were flowed in each channel and incubated for 10 min. After this step, the NeutrAvidin and sample solutions were added in the same way as for the regular PEG slides. A pure DT20 surface was made without embedded BSA or NeutrAvidin by skipping the steps of biotinylated BSA and NeutrAvidin incubation. A detailed protocol is available (**Supplementary Protocol**).

Nonspecific-binding tests. Nonspecific binding on the PEG or DT20 surface was tested by imaging the slide surface and counting the fluorescence spots per imaging area (2,500 μm^2) at varying concentrations of fluorophore-labeled biomolecules (proteins or nucleic acids). Unless specified otherwise, the biomolecules were incubated in the flow chamber for 3–5 min, depending on the biomolecules, before they were washed out by 150 µl T50 buffer followed by 50 µl imaging buffer (T50 buffer containing additional 4 mM Trolox, 0.8% (w/v) glucose, 165 U/ml glucose oxidase and 2170 U/ml catalase)[22]. The same incubation time was applied to the PEG and DT20 surfaces. For nonspecific-binding tests of four ribosomal proteins, five random areas spreading the entire flow channels were imaged; for the rest of the biomolecules, 10–20 random areas were imaged. The average and s.d. of surface spot counts were used as the indicator of the level of nonspecific binding. All the experiments were performed at room temperature (22 ± 1 °C).

DinB was labeled with Cy5 hydrazide (GE Healthcare) through aldehyde tags[14]. Nonspecific-binding tests with or without NeutrAvidin on the surface were conducted in T50 buffer. T50 buffer (pH 8.0) was used in all nonspecific-binding tests unless specified otherwise. Rep was labeled with Cy5 maleimide (GE Healthcare). Four ribosomal proteins (S4, S16, S17 and S20) were labeled with Cy3 maleimide (GE Healthcare), and nonspecific-binding tests were conducted in a buffer containing 80 mM K-HEPES, 300 mM KCl and 20 mM $MgCl_2$ at pH 7.6. IgG #1 was a donkey anti-rabbit antibody (611-701-127, Rockland) labeled with Alexa 647 NHS ester (Invitrogen), and IgG #2 was an Alexa 568–labeled goat anti-mouse antibody (A-11004, Invitrogen). Cy3-labeled ssDNA (34 nt) was purchased from IDT with the sequence of 5′-/Cy3/CAGAATCCGGCTAGTACCTCAATATAGACTCCCT-3′. Nonspecific-binding tests of Cy3-ssDNA (34 nt) were also conducted at pH 7.1 (in addition to pH 8.0). ssDNA (18 nt) was purchased from IDT with the sequence of 5′-/5AmMC6/GCCTCGCTGCCGTCGCCA/3biotin/-3′. This ssDNA (18 nt) was separately labeled with three different fluorophores, i.e., Cy5 NHS ester (GE Healthcare), Abberior Star 635 NHS ester (Abberior) and Atto 647N NHS ester (Sigma).

Prism-based total-internal-reflection fluorescence (TIRF) imaging. The flow chamber was imaged under a prism-based TIRF microscope[23] equipped with a 532-nm laser (Compass 315M, Coherent) and 633-nm laser (Research Electro-Optics) for Cy3 and Cy5 excitation, respectively. The fluorescence collected by a water-immersion objective (60×/1.2 numerical aperture (NA); Olympus) was split into two channels by a dichroic beam splitter and recorded by electron-multiplying charge-coupled device (EMCCD) camera (IXon 897, Andor Technology) with the time resolution of 0.03 s or 0.1 s. The fluorescence emission filters used were a double-notch filter (Z532/633, Chroma) and a band-pass filter (680 ± 20 nm, Chroma).

An averaged image of the first ten camera frames was generated by a custom IDL code, and the fluorescence spots in the averaged image were identified and counted on the basis of two criteria: (i) the fluorescence spot should be fit to a two-dimensional Gaussian within a predetermined fitting error to avoid including multiple molecules or aggregations in the analysis; and (ii) the intensity maxima should be greater than a predetermined threshold. The intensity threshold was kept the same for direct comparison between different surfaces. Some custom software and codes are available at https://cplc.illinois.edu/software and http://bio.physics.illinois.edu/HaMMy.asp; the rest are available upon request.

Preparation of the four ribosomal proteins. *Escherichia coli* ribosomal protein S4 was labeled at residue 189 by site-directed mutagenesis of pET24b/rpS4_C32S as previously described[20]. Single cysteine residues were introduced in *E. coli* ribosomal proteins S16 (position 44) and S20 (position 23) through site-directed mutagenesis (QuikChange, Stratagene) of pET24b/rpS16 and pET24b/rpS20 vectors, respectively[24]. Similarly, a natural cysteine in S17 was replaced with alanine (rpS17:C64A). These variant ribosomal proteins with single cysteine residues were overexpressed and purified by cation-exchange chromatography using an UNO S6 column (Bio-Rad) as described[24]. Isolated proteins were dialyzed overnight into storage buffer 1 (80 mM K-HEPES, pH 7.6, 1 M KCl, 1 mM TCEP) with three buffer changes and stored at −80 °C in 500-µl aliquots.

Purified proteins were preincubated in 1 ml of reaction buffer (80 mM K-HEPES, pH 7.6, 1 M KCl, 1 mM TCEP, 3 M urea) at 20 °C for 30 min and then reacted with a sixfold molar excess of maleimide-linked Cy3 or Cy5 (GE Healthcare) at 20 °C for

another 2 h. The reactions were quenched by adding 50 ml 20 mM Tris-HCl, pH 7.0, 6 M urea and 6 mM 2-mercaptoethanol (20 mM KCl, final concentration). Excess unreacted dye was removed by ion-exchange chromatography. Labeled proteins were dialyzed overnight against storage buffer 2 (80 mM K-HEPES, pH 7.6, 1 M KCl, 6 mM 2-mercaptoethanol) and stored at −80 °C in a light-tight box. The concentration of the labeled proteins was determined from the absorbance at the absorption maxima for the respective cyanine dyes ($\varepsilon_{650,\ Cy5}$ = 250,000 M^{-1} cm^{-1}; $\varepsilon_{550,\ Cy3}$ = 150,000 M^{-1} cm^{-1}).

Single-molecule imaging by STED microscope. A flow chamber passivated by either PEG or DT20 was prepared as described earlier except that it did not have biotin and that, for some experiments (**Fig. 1d** and **Supplementary Fig. 7a**), Alexa 594–labeled streptavidin with ~2:1 labeling ratio (S-32356, Invitrogen; hereinafter SA-A594) was first immobilized nonspecifically to the DDS surface before 0.2% Tween-20 in T50 buffer was added to passivate the surface. Confocal and STED imaging was performed with (**Fig. 1d**,**e**) or without 100 nM SA-A594 in solution, and with 50 nM Alexa 594–labeled protein G B1 domain in solution (**Supplementary Fig. 7**). For each condition, at least three random areas spreading the entire flow channels were imaged.

A custom-built STED microscope was used[15]. Light from a Ti:sapphire laser (λ = 750 nm, Spectra Physics) was split to use as STED and excitation beams. The excitation pulses were generated by a photonic crystal fiber (NKT photonics)[25] and spectrally filtered in the range of 565 ± 12 nm (Semrock). The STED pulses were stretched to ~300 ps by two glass rods (Casix) and a 100-m-long fiber (OZ optics). The spatially filtered excitation and STED pulses were reflected by dichroic beam splitters (Chroma) with circular polarization (B. Halle Nachfl.) and focused onto the sample plane by an objective lens (NA 1.4 HCX PL APO 100×, Leica Microsystems). The lateral doughnut-shaped STED beam was made by a phase plate with a helical lamp pattern (RPC Photonics). The fluorescence signal was collected by the same objective over the wavelength range of 600–640 nm (Chroma) and registered by an avalanche photodiode (PerkinElmer) with a multimode fiber (Thorlabs). The scanning of the sample was accomplished by a piezo stage, and the laser powers of excitation and STED beam were 1.5 μW and 54 mW, respectively.

Holliday junction dynamics. The Holliday junction (HJ) was annealed by mixing four DNA strands (ordered from IDT) with the molar ratio 1:1:1:1 (final concentration, ~10 μM each) in 10 mM Tris-HCl (pH 8.0) and 50 mM NaCl followed by slow cooling from 90 °C to room temperature for ~2 h. The sequences of the four oligonucleotides are as follows: 5′-CCTCCCTAGCAAGCCGCT GCTACGG-3′; 5′-/Cy3/CCGTAGCAGCGCGAGCGGTGGG-3′; 5′-/biotin/CCCACCGCTCGGCTCAACTGGG-3′; 5′-CCCAGT TGAGCGCTTGCTAGGG/Cy5/-3′.

150–250 pM of Cy3- and Cy5-labeled HJ molecules were immobilized on either the PEG surface or DT20 surface. Surface immobilization was mediated by biotin-NeutrAvidin binding between biotinylated HJ, NeutrAvidin and surface-immobilized biotinylated BSA. Excess unbound HJ was flushed out of the sample chamber using 200 μl imaging buffer (20 mM Tris (pH 8.0), 10–80 mM $MgCl_2$, 5 mM NaCl, 4 mM Trolox, 0.8% (w/v) glucose, 165 U/ml glucose oxidase and 2,170 U/ml catalase), and Cy3 and Cy5 intensities from single HJ were recorded by the TIRF microscope[23] with a time resolution of 0.03 s. More than 8,000 molecules were used to construct each histogram, and more than 500 time intervals were used to calculate each transition rate.

PcrA repetitive looping activity. The sequence of the partial duplex DNA used in this experiment is 5′-/Cy3/$(dT)_{40}$GCCTCG CTGCCGTCGCCA-3′+5′-/Cy5/TGGCGACGGCAGCGAGGC/ biotin/-3′ (IDT). PcrA was purified from *Bacillus stearothermophilus* as described[26]. 100 pM PcrA reaction solution was prepared by diluting PcrA stock into imaging buffer (20 mM Tris (pH 8.0), 4 mM Trolox, 0.8% (w/v) glucose, 165 U/ml glucose oxidase and 2,170 U/ml catalase) with additional 10 mM KCl, 5 mM $MgCl_2$ and ATP at either 10 or 500 μM. Then this reaction solution was added into the chamber with surface-immobilized partial duplex DNA. The experiment was performed at room temperature, and the images were recorded by the TIRF microscope[23] with a time resolution of 0.03 s. More than 800 cycles of repetitive FRET changes were used to construct each histogram.

DinB-PCNA binding. *Methanosarcina acetivorans* PCNA, RFC (replication factor C) and DinB were expressed recombinantly in *E. coli* and purified as described previously[14,27]. The DinB we used in this study contained an aldehyde tag at the N terminus and was labeled quantitatively with Cy3 hydrazide using the protocol we published recently[14].

First, Cy5-labeled DNA was added at a concentration of 200 pM, followed by a 5 min incubation and rinse procedure. This DNA construct contained a biotin tag at the 5′ end of the primer, a template of $(dT)_{20}$ and a four-way junction on the distal side of the template[14]. This addition of DNA was repeated a few more times until the surface was homogeneously covered with DNA. Next, a mixture of 20 nM PCNA, 1 mM ATP and 100 nM RFC was added in a buffer at pH 8.0, referred to as imaging buffer, containing 25 mM Tris, 5 mM $MgCl_2$, 0.8% (w/v) glucose and 2 mM Trolox, followed by 5 min incubation. After we repeated this step two more times, sample chambers were rinsed extensively with imaging buffer. Last, Cy3-labeled DinB was added into the chamber at a concentration of 4 nM, incubated for 5 min and rinsed with imaging buffer. FRET imaging of individual immobilized molecules of Cy3-labeled DinB and Cy5-labeled DNA was carried out in imaging buffer plus 1.0 mg/ml glucose oxidase and 1,404 U/ml catalase. The TIRF microscope[23] was used to record images at 0.03-s time resolution.

Preparation of the surfaces tested in Supplementary Figure 1. The PEG surface was prepared by following the previous protocols[5]. According to the protocol reported by Revyakin *et al.*[12], a treatment of the PEG surface with 1,7-dichlorooctamethyltetrasiloxane (siloxane, Sigma-Aldrich, 95%) for 16 h gave the PEG-siloxane surface. The PEG-siloxane surface was further passivated by 0.2% Tween-20 or 1% F-127 (Pluronic F-127, low UV absorbance, Invitrogen), which was referred to as the PEG–siloxane–Tween-20 or PEG–siloxane–F-127 surface, respectively. The DDS-coated surface was prepared as described above by treating the clean quartz surface with DDS for ~1–1.5 h. A DDS-coated surface passivated by 0.2% Tween-20 or 1% F-127 was referred to as the DT20 or DDS–F-127 surface[13], respectively. Similarly, when the PEG surface was treated with DDS and further

doi:10.1038/nmeth.3143

passivated by 0.2% Tween-20 or 1% F-127, it was referred to as the PEG–DDS–Tween-20 or PEG–DDS–F-127 surface, respectively. And when the clean quartz surface was treated with siloxane and further passivated by 0.2% Tween-20 or 1% F-127, it was referred to as the siloxane–Tween-20 or siloxane–F-127 surface, respectively.

S4-rRNA complex dynamics measured in Supplementary Figure 12. The RNA-protein system tested is the 5′ domain of the *E. coli* 16S rRNA (nt 21–556, *E. coli* numbering) and the ribosomal protein S4. The 3′ end of the RNA was extended by 38 nt to base-pair with a complementary DNA primer derivatized with Cy5 and biotin. S4 was labeled at residue 189 with Cy3 by introducing mutations C32S and S189C (ref. 20). 10 nM RNA was annealed with 5 nM primer at 70 °C in 80 mM K-HEPES pH 7.6, 300 mM KCl and then folded for 5 min at 37 °C by adding 20 mM $MgCl_2$. Then the complex was diluted 5× in the same buffer and assembled with 5 nM S4 for 5 min at 37 °C. The complex was immobilized on either the DT20 surface or the PEG surface and was imaged by the TIRF microscope[23] with a time resolution of 0.1 s. More than 200 single-molecule traces were used to construct each histogram.

21. Zhuravlev, L.T. *Colloids Surf. A Physicochem. Eng. Asp.* **173**, 1–38 (2000).
22. Rasnik, I., McKinney, S.A. & Ha, T. *Nat. Methods* **3**, 891–893 (2006).
23. Joo, C. & Ha, T. *Single Molecule Techniques: A Laboratory Manual* (eds. Selvin, P. & Ha, T.) Ch. 2, 3–36 (Cold Spring Harbor Laboratory, 2007).
24. Culver, G.M. & Noller, H.F. *Methods Enzymol.* **318**, 446–460 (2000).
25. Han, K.Y., Leslie, B.J., Fei, J., Zhang, J. & Ha, T. *J. Am. Chem. Soc.* **135**, 19033–19038 (2013).
26. Niedziela-Majka, A., Chesnik, M.A., Tomko, E.J. & Lohman, T.M. *J. Biol. Chem.* **282**, 27076–27085 (2007).
27. Chen, Y.-H. *et al. J. Biol. Chem.* **280**, 41852–41863 (2005).